Food Hydrocolloids 111 (2021) 106264

Contents lists available at ScienceDirect

Food Hydrocolloids

journal homepage: http://www.elsevier.com/locate/foodhyd

Electrohydrodynamic encapsulation of eugenol-cyclodextrin complexes in pullulan nanofibers

Asli Celebioglu *, Tamer Uyar *

Department of Fiber Science & Apparel Design, College of Human Ecology, Cornell University, Ithaca, NY, 14853, United States

ARTICLE INFO

Keywords:
Pullulan
Cyclodextrin
Essential oil
Eugenol
Electrospinning
Antioxidant

ABSTRACT

In this report, the inclusion complexes of eugenol-gamma cyclodextrin (γCD) were incorporated in pullulan nanofibers using electrospinning technique. As a control sample, the pristine eugenol contained pullulan nanofibers were electrospun, as well. The nanofibrous webs were prepared with the initial eugenol content of 12% (w/w) and pullulan/eugenol-γCD nanofibers could preserve ~93% of this volatile essential oil compound due to inclusion complexation. On the other hand, only ~23% of eugenol was preserved in case of pullulan/eugenol nanofibers. The inclusion complexation also provided an enhanced thermal stability for eugenol and its volatilization shifted from ~50-190 °C to ~125–300 °C in case of pullulan/eugenol-γCD nanofibers. The antioxidant performance of eugenol was not affected by the inclusion complexation and the nanofibers of pullulan/eugenol-γCD and pullulan/eugenol indicated ~100% and ~58% radical scavenging activity for the same nanofiber concentration (250 μm/mL). Moreover, pullulan/eugenol-γCD nanofibers maintained the antioxidant activity even after 3-months storage at room temperature (~98%) and heat-treatment performed at 175 °C for 1 h (~93%). The time dependent release test indicated that pullulan/eugenol-γCD nanofibers has a release profile in a relatively controlled manner compared to pullulan/eugenol nanofibers under the same experimental conditions. Here, the functional nanofibrous web encapsulated an essential oil compound was developed using the edible pullulan and non-toxic and natural cyclodextrin molecules. Therefore, pullulan/eugenol-γCD nanofibers can be quite a promising encapsulation and carrying matrix for the essential oils which are widely used in both food and pharmaceutical areas.

1. Introduction

In today's world, there is a growing interest in both food and pharmaceutical industries for developing encapsulation technologies from renewable sources with the intention of packaging, protection, carrying and delivery of active compounds. Biopolymers has become prominent as an alternative for the fossil fuel-based products owing to their non-toxic, sustainable, biodegradable and biocompatible properties (Zhu, Romain, & Williams, 2016). Polysaccharides are one of the most abundant types of biopolymers which are created in the organism of plants, animals and microorganism and therefore extensively supplied in the nature (Yadav & Karthikeyan, 2019). Recently, the polysaccharides being used in the food or pharmaceutical industries are mainly originated from plant and animal sources (Hassan, Chatha, Hussain, Zia, & Akhtar, 2018; Yadav & Karthikeyan, 2019). Nevertheless, microorganism-based polysaccharides are considered to be an emerging biopolymer with their unique properties (Jindal & Khattar, 2018). Pullulan is an attractive type of microbial polysaccharides which can be industrially produced by using fungus-like yeast *Aureobasidium* pullulans in the fermentation process of starch syrup (Sugumaran & Ponnusami, 2017). Pullulan has a linear polymer chain structure which consist of maltotriose units (three α-(1, 4) linked glucose units) connected by α-(1, 6) glycosidic bonds. The distinctive properties of pullulan have received great attention from the food, pharmaceutical, and cosmetic areas, since it is edible, odorless, tasteless, non-mutagenic, neutral, non-hygroscopic and water-soluble biopolymer (Singh, Kaur, & Kennedy, 2019, 2015; Singh, Kaur, Rana, & Kennedy, 2017). Pullulan has been widely utilized as gelling agent, adhesive binder, thickener, solubility enhancer and so on for the mentioned application areas (Sugumaran & Ponnusami, 2017). Most of polysaccharides have branched and complex structures with high diversity causing difficulties during their processing, and so additional chemical modification might be required to eliminate these challenges (Jindal & Khattar, 2018). On the other hand, pullulan has remarkable film and fiber forming

* Corresponding authors.
E-mail addresses: ac2873@cornell.edu (A. Celebioglu), tu46@cornell.edu (T. Uyar).

https://doi.org/10.1016/j.foodhyd.2020.106264
Received 21 May 2020; Received in revised form 18 July 2020; Accepted 17 August 2020
Available online 18 August 2020

properties due to its stair step type macromolecular structure and this makes easy to utilize pullulan as coating and packaging materials (Trinetta & Cutter, 2016). This special linage structure, water solubility and the specific rheological properties enable the electrospinning of pullulan into homogenous and defect-free nanofibrous web structures without using any toxic or aggressive solvent systems (Stijnman, Bodnar, & Tromp, 2011). Even, it has been reported that pullulan can be used in order to enhance the electrospinnability of the problematic electrospinning systems by modifying the viscosity, conductivity and surface tension (Qin, Jia, Liu, Kong, & Wang, 2019; Stijnman et al., 2011).

Previous studies have shown the versatility of pullulan nanofibers to encapsulate wide range of bioactive compounds for the potential food and pharmaceutical practices. With respect to encapsulation for food applications, the food-grade electrospun nanofibrous webs have been obtained by the incorporation of fish oil (García-Moreno et al., 2017), folic acid (Aceituno-Medina, Mendoza, Lagaron, & López-Rubio, 2015), nisin (Soto, Hernández-Iturriaga, Loarca-Piña, Luna-Bárcenas, & Mendoza, 2019), tea phenols (Shao, Niu, Chen, & Sun, 2018), resveratrol (Seethu et al., 2020), curcumin (Blanco-Padilla, López-Rubio, Loarca-Pina, Gómez-Mascaraque, & Mendoza, 2015) into the blended nanofibrous webs of pullulan and biopolymers of dextran, carboxymethyl cellulose and isolate protein of amaranth and whey. From the point of pharmaceutical practices, there are several studies reporting the utilization of the functionalized pullulan based electrospun nanofibers for the purpose of fast dissolving oral drug delivery (Qin et al., 2019), ocular drug delivery (Göttel et al., 2020) and antibacterial/antimicrobial (Islam & Yeum, 2013; Román et al., 2019) applications. The advantages of pullulan rising from its structural properties; biocompatibility and processability make this polymer an attractive alternative among other commercial polymer types for the further development of functional nanofibrous webs which might be utilized in food and pharmaceutical areas.

The electrohydrodynamic atomization method of electrospinning is a feasible, flexible, and cost-effective alternative to fabricate an encapsulation matrix for various food additives and pharmaceutical molecules accompanied with many functional and structural advantages (Jain, Shetty, & Yadav, 2020; Xue, Wu, Dai, & Xia, 2019). The major features that make electrospinning attractive are the large surface area, 3D continuous structure and high porosity of the ultimate electrospun nanofibers (Xue et al., 2019). Moreover, it enables the manipulation of the nanowebs properties by introducing different functional components, and finally superior and inclusive properties are attained while sustaining the primitive qualities of each component (Xue et al., 2019). The manipulation flexibility of nanofibers has generated demand for the large-scale production in different industries. Therefore, various recent methods have been emerged to reach higher productivity rate such as multi-nozzle, needless, airblowing-assisted, corona, pressurized gyration and centrifugal spinning (Alenezi, Cam, & Edirisinghe, 2019; Duan & Greiner, 2019; Farkas et al., 2019; Mahalingam, Homer-Vanniasinkam, & Edirisinghe, 2019; Xue et al., 2019). It is noteworthy that the conditions of simple electrospinning can be adapted and modified for the mentioned scale-up production techniques to fabricate analogous nanofibrous structures. Differently from other encapsulation technique (e.g. spray drying), film formation processes (e.g. extrusion) or melt spinning, electrospinning process is performed at ambient conditions which makes it also more feasible for the encapsulation of thermally sensitive and volatile compounds. From this point of view, it has been thought that the electrospinning might be also conducted for the efficient encapsulation of essential oils into nanofibrous webs.

Essential oils are the mixture of hydrophobic volatile compounds having valuable properties including fragrance, antioxidant, antiseptic, antibacterial, antifungal and anti-inflammatory (Amorati, Foti, & Valgimigli, 2013). Due to their assorted properties and relatively safe status, essential oils are of great interest for the food, medical and cosmetic industries (Amorati et al., 2013; Llana-Ruiz-Cabello et al., 2015). Eugenol (2-methoxy-4-(2-propenyl) phenol) is one of the major components of clove essential oil and has an inhibitor effect on the oxidative stress due to its radical scavenging property (Bezerra, Militão, De Morais, & De Sousa, 2017). As in most of components of essential oils, the encapsulation, preservation, and the release of eugenol also displays a main challenge when considered its sensitivity to heat (Wadhwa, Kumar, Chhabra, Mahant, & Rao, 2017). By means of previously mentioned advantages, electrospinning technique seems appropriate to encapsulate the essential oils in the carrier matrix of electrospun nanowebs. However, most of the polymer types can fall short of preserving the essential oils during electrospinning process and they may alone not be sufficient to encapsulate these compounds because of the high volatility and fugacity of essential oils. There are different reports in the literature that address the functionalization of electrospun nanofibers with the cyclodextrin inclusion complexes of these hydrophobic compounds to figure this problem out (Celebioglu, Yildiz, & Uyar, 2018b, Celebioglu et al., 2018a; Celebioglu et al., 2018c; Yildiz, Celebioglu, Kilic, Durgun, & Uyar, 2018).

Cyclodextrin (CD) is a type of oligosaccharides having cyclic and truncated molecular structure and capable of forming inclusion complexes with a variety of compounds by capturing into its hydrophobic cavity (Bilensoy, 2011). The thermal/oxidative stabilization, enhanced water solubility and the controlled/delayed release profiles incident to inclusion complexation open the way for various active compound to be effectively used in different areas including food, pharmacy, cosmetic, textile etc. (Bilensoy, 2011; Sharma & Baldi, 2016). In one of the related studies, Mascheroni et al. indicated the one-step fabrication of edible polysaccharide system composed of pullulan and the CD inclusion complexes of an aroma compound for evaluating the humidity based release profile (Mascheroni et al., 2013). In this work, we have developed an efficient encapsulation and carrying platform for one of the most widely used essential oil compound in the form of flexible and free-standing nanofibrous webs by using a sustainable polymer source and an additional natural complexation agent. Herewith, we have fabricated eugenol-γCD inclusion complex incorporated pullulan nanofibers in one-step process (Fig. 1). The superiority of this edible polysaccharides-based system compared to pure eugenol included pullulan nanofibers were investigated using different characterization techniques. The antioxidant performance of the nanofibrous webs were comparatively evaluated for both long-term stored and heat-treated samples, as well.

2. Materials and methods

2.1. Materials

Pullulan (Mw: 300 000 g/mol, TCI America), eugenol (99% purity, Acros Organics), deuterated dimethylsulfoxide (DMSO-d_6, 99.8%, Cambridge Isotope), 2,2-diphenyl-1-picrylhydrazyl (DPPH, ≥97%, TCI America), dimethyl sulfoxide (DMSO, > 99.9%, Sigma Aldrich) and methanol (≥99.8% (GC), Sigma Aldrich) were provided commercially. Gamma cyclodextrin (γCD, Cavamax W8 Food) is a kind gift from Wacker Chemie AG (USA) for scientific studies. Purification was not carried out for any chemicals. The required water was supplied from Millipore Milli-Q ultrapure water system (Millipore, USA).

2.2. Methods

2.2.1. Preparation of eugenol-γCD inclusion complexes and electrospinning systems

The inclusion complexes of eugenol and γCD were prepared using the 2:1 M ratio (eugenol:CD). Firstly, γCD (23% w/v) was dissolved in water, then eugenol was added to the aqueous solution of γCD. The system was stirred overnight at room temperature and highly turbid inclusion complex dispersion was obtained. The pullulan (20%, w/v) was subsequently added to the eugenol-γCD inclusion complex system

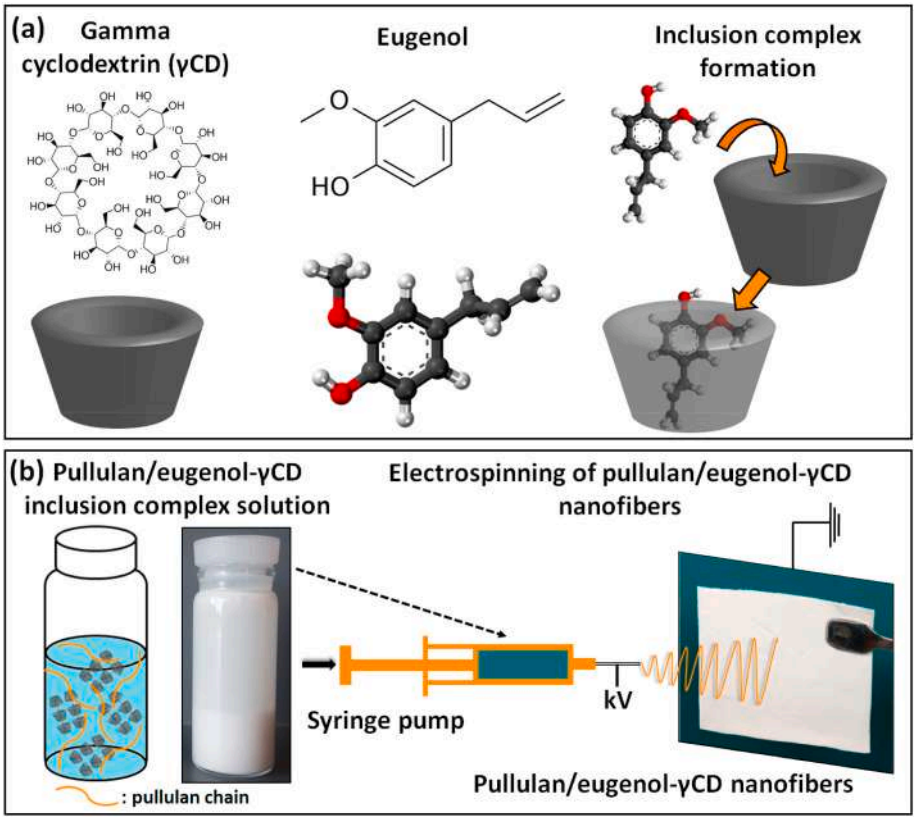

Fig. 1. (a) The chemical structure of γCD and eugenol. The schematic representation of inclusion complex formation between γCD and eugenol. (b) The schematic representation of the electrospinning of pullulan/eugenol-γCD nanofibers.

and stirred until the polymer dissolved (room temperature). As control samples, pure pullulan and pullulan/eugenol solutions were prepared, as well. For all systems, the pullulan concentration was fixed as 20% (w/v, with respect to solvent) and the eugenol content was set to ~ 12% (w/w, with respect to total sample amount) for pullulan/eugenol and pullulan/eugenol-γCD systems. Before electrospinning, conductivity, and viscosity of all solutions (pullulan, pullulan/eugenol, and pullulan/eugenol- γCD) were determined using proper techniques. The conductivity of the solutions was measured by Conductivity-meter (FiveEasy, Mettler Toledo, USA) at room temperature. The viscosity of the same systems was recorded at the range of 0.01–1000 s^{-1} (shear rate) by a rheometer (AR 2000 rheometer, TA Instrument, USA) equipped with CP 20-4 spindle (4°). The electrospinning equipment (Spingenix, model: SG100, Palo Alto, USA) has been used to form electrospun nanofibers. For this, all aqueous systems were separately loaded into 3 mL syringes which were right after located horizontally to the syringe pump. The high voltage (15 kV) was supplied to the tip of the stainless-steel needle (27G) which were fixed to the syringes. Concurrently, the electrospinning solution was pumped through the needle using syringe pump with a stable flow rate (0.5 mL/h). For the deposition of nanofibers, a metal plate covered with a piece of Al foil was placed 15 cm away from the needle. The environmental conditions of humidity and temperature were recorded as ~25% and ~20 °C, respectively during the process.

2.2.2. Morphology analysis

The morphology of pullulan, pullulan/eugenol and pullulan/eugenol-γCD nanofibers were explored using scanning electron microscopy (SEM, Tescan-MIRA3, Czechia). Since the samples do not have conductive nature, they create charging problem during the SEM measurements. Therefore, all samples were coated with a thin layer of Au/Pd prior the measurements using sputter coating under vacuum. At least 100 nanofibers were included for the calculation of the average diameter (AD, mean ± standard deviation) of fibers using SEM images (ImageJ software).

2.2.3. The Fourier transform infrared spectroscopy

The attenuated total reflectance Fourier transform infrared spectrometer (ATR-FTIR, PerkinElmer, USA) was used to get the FTIR spectra of eugenol, γCD, pullulan nanofibers, pullulan/eugenol nanofibers and pullulan/eugenol-γCD nanofibers. The absorption mode of FTIR spectra were recorded at 4000-600 cm^{-1} (resolution of 4 cm^{-1}) by 64 scans.

2.2.4. Proton nuclear magnetic resonance spectroscopy

Proton nuclear magnetic resonance (^{1}H NMR) measurements were utilized in order to reveal the existence of eugenol and to calculate roughly its content in the samples. ^{1}H NMR measurements were performed using magnetic resonance spectrometer equipped with autosampler (NMR, Bruker AV500, USA). For the measurements, eugenol, γCD, pullulan nanofibers, pullulan/eugenol nanofibers and pullulan/eugenol/γCD nanofibers were dissolved in DMSO-d_6 (60 mg/mL). The ^{1}H NMR measurements were ended by 16 scans. The ^{1}H NMR spectrum of each sample was plotted with chemical shifts (δ) values in ppm (parts per million) (external standard of TSP signal (0 ppm)) and processed using the software of Mestranova. For the calculations, the distinct peaks of components were considered, the integration of the considered peaks were proportioned, and the results were obtained in terms of molar ratio which can be easily converted to % (w/w, with respect to total sample amount).

2.2.5. X-ray diffraction

X-ray diffractometer (Bruker D8 Advance ECO, USA) was conducted to determine the X-ray diffraction patterns of γCD, pullulan nanofibers, pullulan/eugenol nanofibers and pullulan/eugenol-γCD nanofibers. The

XRD scanning was performed using Cu Kα radiation in the 2θ range of 5°–30° (40 kV and 25 mA).

2.2.6. Thermal characterization

Thermal profiles of eugenol, γCD, pullulan nanofibers, pullulan/eugenol nanofibers and pullulan/eugenol-γCD nanofibers were evaluated using two different techniques of thermogravimetric analyzer (TGA, Q500, TA Instruments, USA) and differential scanning calorimeter (DSC, Q2000, TA Instruments, USA). The TGA analyses were performed at 30 °C–600 °C with heating rate of 20 °C/min. For DSC measurements, each sample was precisely weighted into Tzero pan and heated from 0 °C to 240 °C at a heating rate of 10 °C/min. The both thermal analyses of TGA and DSC were performed in inert atmosphere using nitrogen gas.

2.2.7. Encapsulation efficiency test

For the calculations, certain amount of pullulan/eugenol nanofibers and pullulan/eugenol-γCD nanofibers were dissolved in dimethyl sulfoxide (DMSO) and the eugenol content in these samples were determined by UV–Vis-spectroscopy (PerkinElmer, Lambda 35, USA) (284 nm). The calibration curve of eugenol in DMSO showed linearity and acceptability with $R^2 \geq 0.99$. The results were obtained as mean ± standard deviation by the triplicate experiments. The encapsulation efficiency (%) was calculated using the following equation:

$$\text{Encapsulation efficiency } (\%) = \text{Ce/Ct} \times 100 \quad (1)$$

where Ce and Ct are the concentration of loaded eugenol and the initial concentration of eugenol in the nanofibrous sample, respectively. The encapsulation efficiency was also calculated for nanofibrous webs which were stored for 3-months at room temperature or heated at 175 °C for 1 h.

2.2.8. Time dependent release test

For the release test, same amount of pullulan/eugenol and pullulan/eugenol-γCD nanofibers (~60 mg) and 40 mL of distilled water were used. Here, samples were separately positioned in a beaker and aqueous medium was poured subsequently. The incubator shaker was used to shake beakers at the speed of 230 rpm (at room temperature). For UV–Vis measurements, 0.5 mL of the aliquot was withdrawn from the release system and 0.5 mL of fresh water was put at the definite time points. For calculations, the maximum absorbance intensity of eugenol at 284 nm was considered. The calibration curve ($R^2 \geq 0.99$) was conducted to adapt measurements results to the concentration (μg/mg). Mathematical models were used (zero and first-order release model, Higuchi release model and Korsmeyer-Peppas equation (see supporting information)) in order to examine the kinetic profile of samples (Peppas & Narasimhan, 2014).

2.2.9. Antioxidant activity test

The concentration dependent antioxidant activity of pullulan/eugenol nanofibers and pullulan/eugenol-γCD nanofibers were examined using 2,2-diphenyl-1-picrylhydrazyl (DPPH) radical scavenging assay. For this, the aqueous solutions of both samples were prepared at the concentration range of 4–250 μg/mL. Then, the aqueous solutions having different sample concentration were separately mixed with the freshly prepared methanolic solution of DPPH (75 μM) so as to obtain 1:6 (sample:DPPH) volume ratio. After incubation in the dark for 10 min, the attenuation of the DPPH absorption intensity (517 nm) was examined for all samples using UV–Vis spectroscopy. As control, the same experiment was carried out for pristine pullulan nanofibers and γCD powder, as well. The antioxidant activity was also examined for pullulan/eugenol and pullulan/eugenol-γCD nanofibers which were stored for 3-months at room temperature or heated at 175 °C for 1 h. For these experiments, the aqueous solutions of samples were prepared by the highest sample concentration of 250 μg/mL which was also used for concentration dependent test. All experiments were performed for three times and the results were expressed as mean ± standard deviation. The radical scavenging efficiency of samples were calculated in terms of inhibition percentage by using the following equation:

$$\text{Inhibition } (\%) = (A_{control} - A_{sample})/A_{control} \times 100 \quad (2)$$

where A_{sample} stands for the absorbance values of sample solution and $A_{control}$ stands for the control DPPH solution one. The 50% inhibition (IC50) concentrations was also determined from the concentration dependent graph in order to demonstrate the essential amount of sample to decrease the DPPH absorbance by 50% (Ak & Gülçin, 2008).

2.2.10. Statistical analyses

All replicated experiment results ($n \geq 3$) were represented as mean values ± standard deviations. The one-way/two-way of variance (ANOVA) were carried out and OriginLab (Origin 2019; USA) was utilized for this purpose (0.05 level of probability).

3. Results and discussion

3.1. Morphology characterization

In the previous reports related to inclusion complex formation between eugenol and cyclodextrin (CD), it was found that, γCD is the most favorable one for the inclusion complex formation among other CD types due to better size match (Kayaci, Ertas, & Uyar, 2013; Song, Xu, Wang, & Yang, 2009). Additionally, the higher solubility of γCD (23%, w/v) compared to other native CD types (αCD and βCD) can enable to prepare aqueous system with higher inclusion complex concentration and this can offer an advantage for the one-step electrospinning of inclusion complexes incorporated nanofibers with higher amounts of active compounds. In this study, the electrospinning of eugenol-γCD inclusion complex encapsulated nanofibers was performed in one-step. For this, pullulan polymer (20%, w/v) was directly dissolved into the aqueous eugenol-γCD inclusion complex suspension and electrospinning were performed afterwards. The pristine pullulan and eugenol loaded pullulan solutions were also prepared as control samples. For each system, pullulan, γCD and eugenol concentrations were summarized in Table 1. As is seen in Fig. 2, the clear solution of pullulan has been into turbid and white form in case of pullulan/eugenol and pullulan/eugenol-γCD systems because of the emulsion of eugenol and the suspension of eugenol-γCD inclusion complex crystals, respectively. The free-standing nanofibrous webs were successfully fabricated from all aqueous systems of pullulan, pullulan/eugenol and pullulan/eugenol-γCD (Fig. 2). In Fig. 2, the representative SEM images of sample were given. Here, pullulan and pullulan/eugenol nanofibrous webs had uniform and defect-free morphology and the inclusion complex crystals were randomly distributed through the pullulan/eugenol-γCD nanofibrous

Table 1
The solution properties and the fiber diameters of resulting electrospun nanofibers.

sample[a]	γCD conc. (%, w/v)[b]	eugenol conc. (%, w/w)[c]	viscosity (Pa·s)	conductivity (μS/cm)	average diameter (nm)
pullulan	–	–	0.81	44.7	385 ± 70
pullulan/eugenol	–	11.9	1.51	45.4	525 ± 125
pullulan/eugenol-γCD	23	11.7	0.82	64.6	265 ± 80

[a] Pullulan concentration is 20% (w/v, with respect to solvent volume) for each system.
[b] With respect to solvent volume (water).
[c] With respect to total sample amount.

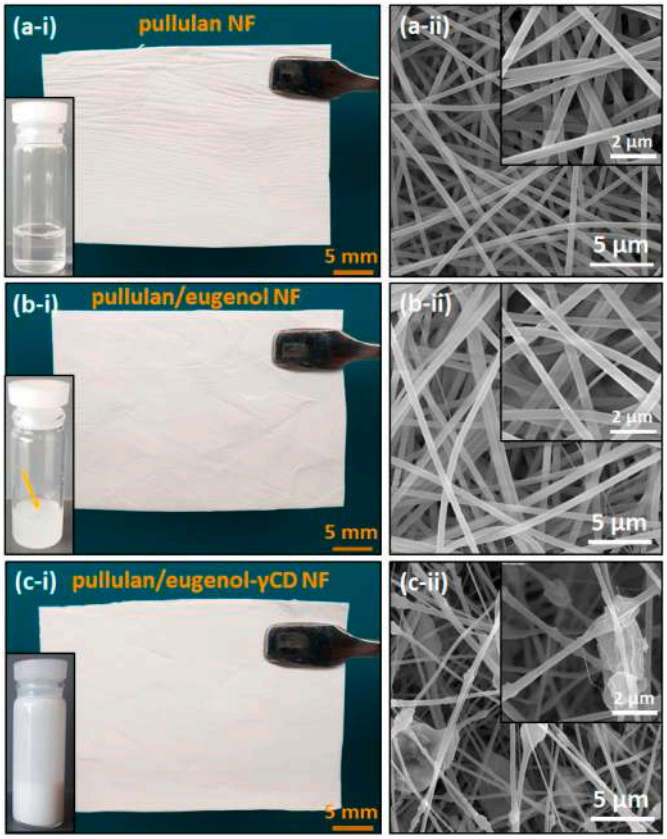

Fig. 2. (i) The photographs of electrospinning solutions and the ultimate nanofibrous webs and (ii) SEM images of (a) pullulan nanofibers (NF), (b) pullulan/eugenol nanofibers (NF) and (c) pullulan/eugenol-γCD nanofibers (NF).

webs. The electrospun nanofibers had fiber size in the range of ~80–700 nm with varying average dimeter (AD) values (Table 1). The viscosity and the conductivity of the electrospinning solutions are the main elements which influence the morphology and the size of the fibers (Uyar & Besenbacher, 2008; Xue et al., 2019). Table 1 indicated that the pullulan solution had a conductivity approximating that of the pullulan/eugenol system. On the other hand, the viscosity of the pullulan solution increased by the addition of eugenol. This finding explained the thicker fiber formation for pullulan/eugenol system (525 ± 125 nm) when compared to pullulan system (385 ± 70 nm). Since, the stretching of the electrospinning jet was inhibited by the higher viscosity of pullulan/eugenol solution and thicker fibers were formed compared to pristine pullulan system (Xue et al., 2019). The pullulan/eugenol-γCD system had the highest conductivity compared to others (Table 1) and its viscosity was lower than the pullulan/eugenol solution. Therefore, pullulan/eugenol-γCD nanofibrous webs had the thinnest average fiber size of 265 ± 80 nm compared to other two nanofibrous webs. First of all, the lower viscosity of the pullulan/eugenol-γCD solution ensured higher stretching of the jet during the electrospinning and so resulted in thinner fibers compared to pullulan/eugenol nanofibers. Besides, the highest conductivity of the pullulan/eugenol-γCD system ensured more repulsion of the charges exist at the surface and electrospinning jet was exposed much more stretching which leaded to thinner fiber formation than pullulan and pullulan/eugenol nanofibrous webs. To conclude, these results are correlated with the general findings for the electrospinning procedure in which the conductivity and the viscosity of the solutions are the main parameters determining the morphology and the fiber size of ultimate electrospun nanofibers (Uyar & Besenbacher, 2008; Xue et al., 2019). The statistical analyses supported our results where the significant variations were detected between samples ($p < 0.05$).

3.2. Structural characterization

To examine the existence of eugenol in the electrospun nanofibers, the structural analyses of eugenol, γCD, pullulan nanofibers, pullulan/eugenol nanofibers and pullulan/eugenol-γCD nanofibers were performed using Fourier transform infrared (FTIR) spectroscopy (Fig. 3). For the FTIR spectrum of eugenol, there were distinct absorption bands at 3520 cm^{-1}, 3100-2790 cm^{-1}, 1637 cm^{-1}, 1607 cm^{-1}/1512 cm^{-1}, 1465 cm^{-1}, 1431 cm^{-1}/1366 cm^{-1}, 1264 cm^{-1}/1231 cm^{-1} represented the vibrations of ν(O–H), methyl and methylene ν(C–H), vinyl ν(C═C), aromatic ν(C═C), methylene δ_s(C–H), methyl δ_s(C–H) and δ_{as}(C–H), ν(C–O) and ν(C–O–C) stretching, respectively (Wang, Li, Si, Lin, & Chen, 2011). On the other hand, the spectrum obtained for the γCD indicated dominant stretching bands at 3266 cm^{-1} for symmetrical and asymmetrical stretching of ν(O–H) and 2925 cm^{-1} for stretching of methyl/methylene ν(C–H). The other absorption bands at 1641 cm^{-1}, 1153 cm^{-1} and 1077 cm^{-1}/1020 cm^{-1} corresponded to the H–O–H bending, asymmetric ν(C–O–C) link stretching and the ν(C–O)/ν(C–C) stretching, respectively (Abarca, Rodriguez, Guarda, Galotto, & Bruna, 2016; Wang et al., 2011). Pullulan polymer has maltotriose repeating units which are linked each other with α-(1,6) glycosidic bond and the maltotriose units consist of three glucose units linked by α-(1,4) glycosidic bond (Yang, Xie, Liu, Kong, & Wang, 2020). Hence, the chemical structure of pullulan is quite like γCD which is composed of α-(1,4) linked glucopyranose sub-units (Fig. 1). Therefore, pullulan and γCD had similar FTIR pattern having the analogous absorption bands at the parallel region of spectrum (Fig. 3a). Pristine pullulan nanofibers exhibited absorption peaks located at 3313 cm^{-1}, 2925 cm^{-1} and 1641 cm^{-1} attribute to the ν(O–H) stretching, ν(C–H) stretching and H–O–H bending, respectively (Shao et al., 2018; (Yang et al., 2020). The other intense peaks between 1200 cm^{-1} and 1000 cm^{-1} were due to the ν(C–O) stretching (Islam & Yeum, 2013; Shao et al., 2018) and by the incorporation of eugenol-γCD inclusion complex, the absorption peak of γCD located at the region of 1200 cm^{-1}-1000 cm^{-1} appeared for pullulan/eugenol-γCD nanofibers (Fig. 3b). However, for both pullulan/eugenol and pullulan/eugenol-γCD nanofibers, the peaks of eugenol were not obvious at this given region. Since, the absorption peaks of pullulan and γCD overlapped and dominated the eugenol peaks due to their higher amount compared to eugenol content into both nanofibers (Table 1). On the other hand, FTIR spectra of pullulan/eugenol and pullulan/eugenol-γCD nanofibers had differences compared to pullulan nanofibers. Fig. 3c indicated that, the absorption peaks of eugenol located at 1512 cm^{-1}, 1465 cm^{-1}, 1431 cm^{-1}, 1264 cm^{-1} and 1231 cm^{-1} were observed in case of pullulan/eugenol and pullulan/eugenol-γCD nanofibers confirming the existence of eugenol in both samples. However, eugenol gave higher strength in the spectrum of pullulan/eugenol-γCD nanofibers than pullulan/eugenol nanofibers. As it will be demonstrated by the further analyses and discussed in the following sections (^{1}H NMR and encapsulation efficiency), the reason for the higher absorption strength of eugenol in case of pullulan/eugenol-γCD nanofibers might be the higher content of eugenol which is the result of inclusion complexation. In brief, FTIR findings has indicated the eugenol incorporation into electrospun pullulan/eugenol and pullulan/eugenol-γCD nanofibers.

The structural analysis of pullulan/eugenol and pullulan/eugenol-γCD nanofibers has been also performed using ^{1}H NMR. First of all, the characteristic peaks of eugenol, γCD and pullulan were determined from their ^{1}H NMR spectra. Fig. 4 depicted the chemical structures of eugenol, γCD, pullulan, and ^{1}H NMR spectra of eugenol, γCD powder and the nanofibers of pullulan, pullulan/eugenol, pullulan/eugenol-γCD. ^{1}H NMR findings have also confirmed the presence of eugenol in both pullulan/eugenol and pullulan/eugenol-γCD nanofibers (Fig. 4). Here, it is clear that pullulan/eugenol nanofibers contained lesser amount of eugenol compared to pullulan/eugenol-γCD nanofiber, since the intensity of the eugenol peaks was distinctively lower in case of pullulan/eugenol sample than pullulan/eugenol-γCD one (Fig. 4). It is also worthy

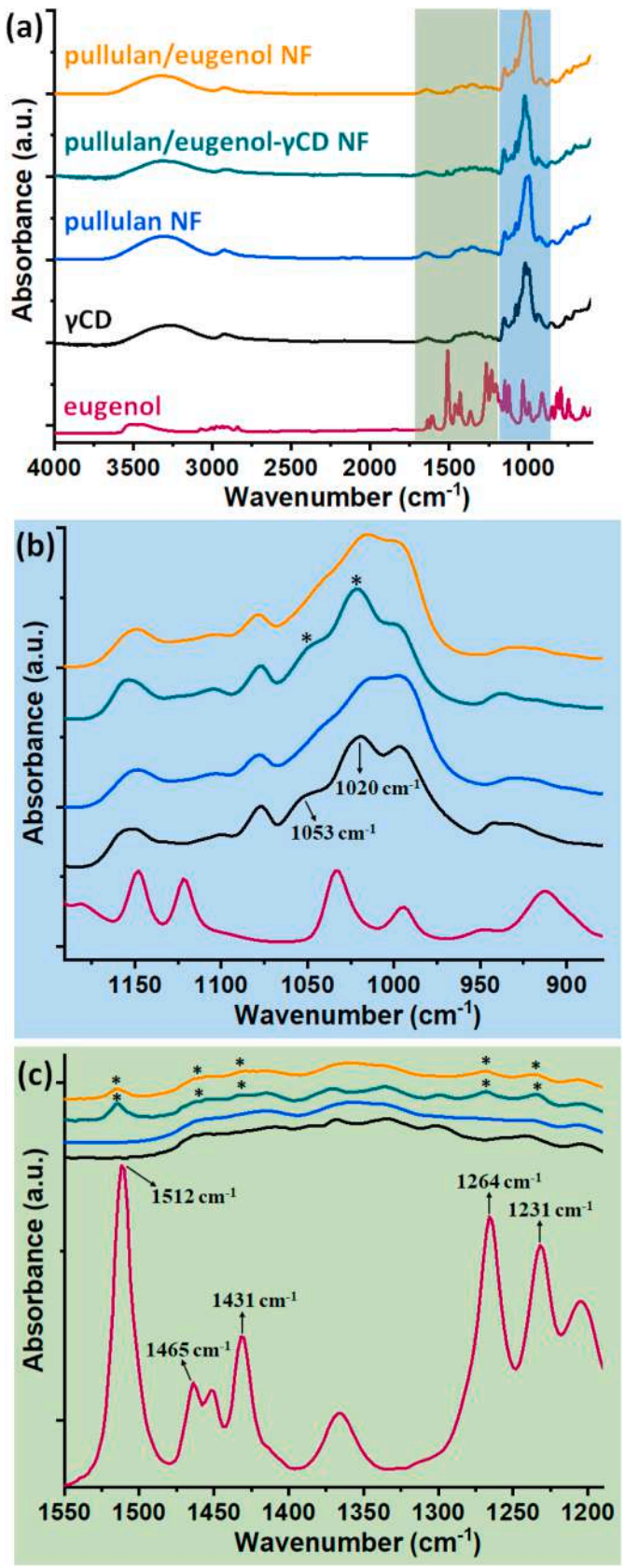

Fig. 3. (a) The full and (b), (c) expanded range FTIR spectra of eugenol, γCD, pullulan nanofibers (NF), pullulan/eugenol-γCD nanofibers (NF) and pullulan/eugenol nanofibers (NF).

to point out, the characteristic shifts of pure eugenol were identically observed at ^{1}H NMR spectra of both nanofibers and this demonstrated that the chemical structure of eugenol was preserved during the whole process of electrospinning. ^{1}H NMR measurement is also a useful approach for the quantitative calculations of the components exist in the samples. Here, the distinct peaks of each component, which were not overlapped with others, were chosen for the calculations. The protons peaks of eugenol, γCD and pullulan located at 6.52–6.76 ppm (H-c,f,e) (Barba, Eguinoa, & Maté, 2015), 5.70–5.83 ppm (OH-2,3) (Kayaci et al., 2013) and 5.32–5.62 ppm (OH-2,3) (Shibata, Asahina, Teramoto, & Yosomiya, 2001), respectively were initially integrated and then proportioned to each other to determine approximate eugenol content in both electrospun nanofibers of pullulan/eugenol and pullulan/eugenol-γCD. Even though, both nanofibers have been initially prepared so as to include the similar amount of eugenol (~12%, w/w), the eugenol content was approximately calculated as ~ 3% and ~11% for pullulan/eugenol and pullulan/eugenol-γCD nanofibers, respectively. These findings have revealed that, while small amount of eugenol was protected in case of pullulan/eugenol nanofibers, the initial amount used for the preparation was substantially preserved for pullulan/eugenol-γCD nanofibers due to inclusion complex formation.

In this study, we have performed the powder X-ray diffractometer (XRD) measurements to examine the crystalline structures of samples. Fig. 5 indicated the XRD pattern of pristine γCD powder, nanofibers of pullulan, pullulan/eugenol and pullulan/eugenol-γCD. The pristine γCD has "cage-type" crystalline structure in which each CD cavity blocks the neighboring CD cavity and this packing form a specific XRD pattern with the characteristic peaks of $2\theta = 5.2$, 12.4, 14.0, 16.5, 18.8 and 21.8° (Fig. 5a). On the other hand, "channel-type" packing can be obtained by the inclusion complexation where the CD stack on top of each other in order to form cylindrical channels (Celebioglu, Ipek, Durgun, & Uyar, 2017) (Fig. 5a). As is seen, the as-received pullulan nanofibers did not exhibit an intense diffraction peak and the broad peak centered at about $2\theta = 18.5°$ was associated with the *d*-spacing of 4.52 Å (Islam & Yeum, 2013; Seethu et al., 2020). Pullulan/eugenol nanofibers represented a similar diffraction pattern with pure pullulan nanofibers, and this proved the distribution of eugenol molecule through the nanofibers without the formation of a specific crystal phase. In case of pullulan/eugenol-γCD nanofibers, the amorphous XRD pattern of pure pullulan was dominated by the distinct diffraction pattern of eugenol-γCD inclusion complexes which are encapsulated through nanofibers. The intense peaks at $2\theta = 7.5$, 12.1, 14.2, 15.0, 15.9, 16.8 and 21.9° shows the "channel-type" packing due to inclusion complex formation between eugenol and γCD (Celebioglu et al., 2017; Kayaci et al., 2013). This finding has supported the SEM analysis in which the crystals of eugenol-γCD inclusion complexes were clearly observed through the nanofiber matrix (Fig. 2).

The thermal behavior of samples was evaluated using thermogravimetric analyzer (TGA). The thermograms of eugenol, γCD powder, nanofibers of pullulan, pullulan/eugenol and pullulan/eugenol-γCD were depicted in Fig. 6a. The volatility of eugenol has been also confirmed by the TGA thermograms in which the weight loss of eugenol started at ~50 °C and its volatilization was completed at ~190 °C (Fig. 6a). In case of γCD powder and pristine pullulan nanofibers, there were two main weight losses: i) the dehydration of water until ~130 °C and ii) the main degradation of samples at ~330 °C. The thermogram of pullulan/eugenol nanofibers showed similarity with the TGA profile of pullulan nanofiber and two distinct weight losses were observed which corresponds to the dehydration of water (until ~ 130 °C) and the major degradation of pullulan (~330 °C). The uncomplex eugenol content was not detected in the TGA thermogram of pullulan/eugenol nanofibers as a separate step (Fig. 6a). First of all, the initial content of eugenol (~12%, w/w (with respect to total sample amount)) could not be preserved and large amount of eugenol was lost during the preparation and electrospinning steps. Additionally, the volatilization step of eugenol and water took place at a very similar temperature region and most probably this

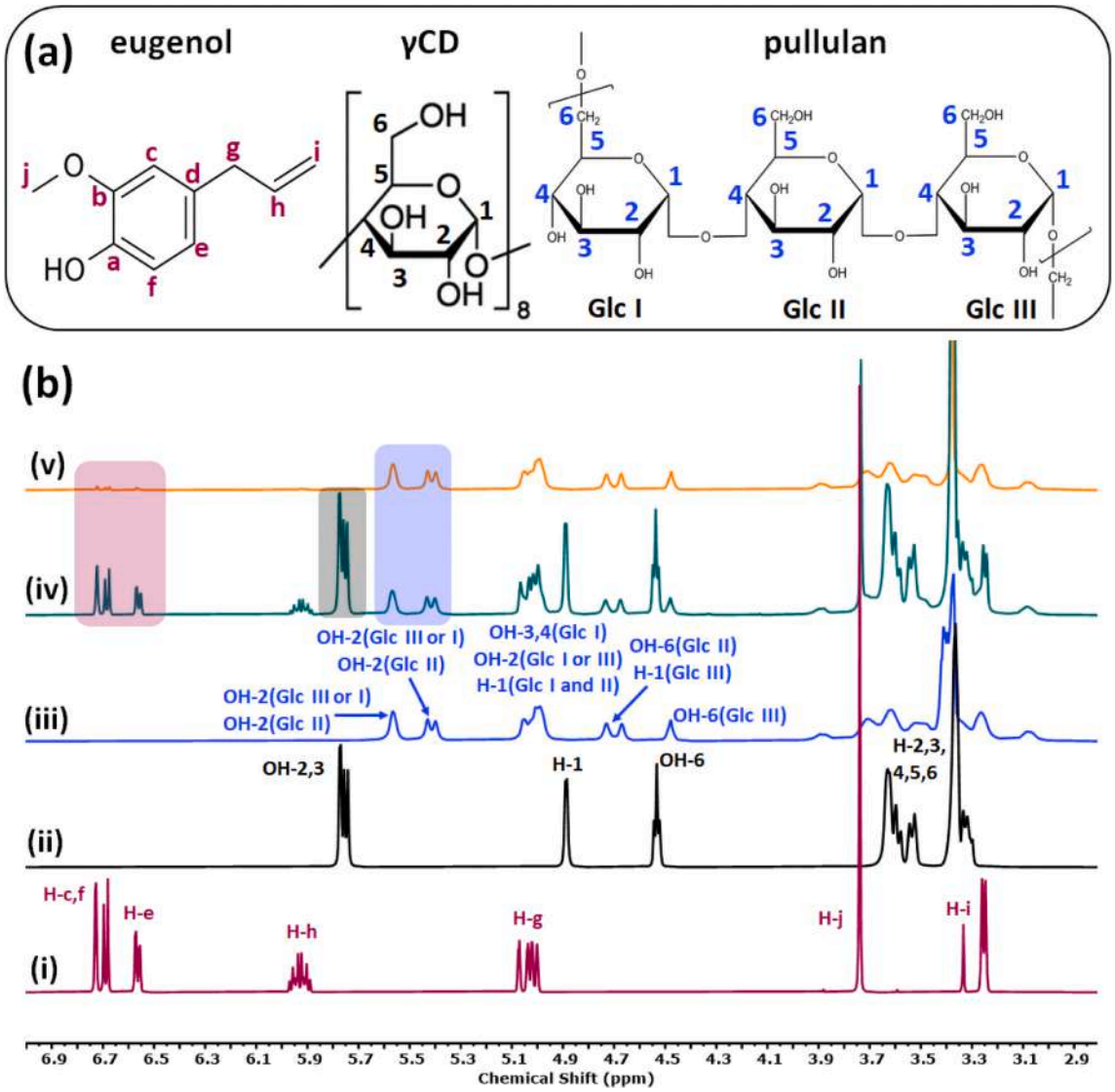

Fig. 4. (a) The chemical structure of eugenol, γCD and pullulan. (b) ^{1}H NMR spectra of (i) eugenol, (ii) γCD, (iii) pullulan nanofibers, (iv) pullulan/eugenol-γCD nanofibers and (v) pullulan/eugenol nanofibers which were recorded by dissolving samples in DMSO-d_6.

disenabled the detection of eugenol and water separately in the thermogram of pullulan/eugenol nanofibers. On the other hand, there were three weight losses in the thermogram of pullulan/eugenol-γCD nanofibers which were due to the water dehydration (~110 °C), volatilization of complexed eugenol (~125 °C–300 °C) and the main degradation of pullulan and γCD (~330 °C) (Fig. 6a). As it was reported previously, the thermal degradation or the evaporation/volatilization of guest molecules can shift to higher temperature upon complexation with CD molecules (Mura, 2015; Wadhwa et al., 2017). Our results supported the previous ones and we have observed that the thermal volatilization of eugenol shifted from the range of ~50–190 °C to ~125–300 °C in case of pullulan/eugenol-γCD nanofibers (Fig. 6a). Here, the interaction with the cavity of γCD leaded to a volatilization process which occurred at the higher temperatures compared to pristine state of eugenol and this demonstrated the significant enhancement of the thermal stability of eugenol by the inclusion complexation. Unlike pullulan/eugenol nanofibers, the approximative eugenol content was determined from the thermogram of pullulan/eugenol-γCD nanofibers and it was calculated as ~10% (w/w, with respect to total sample amount) which was slightly lower than the initial content of eugenol (~12%, w/w) used to prepare the electrospinning solution. Even so, the exact eugenol content of both pullulan/eugenol and pullulan/eugenol-γCD nanofibers was calculated by the further analyses discussed in the following sections.

Differential scanning calorimeter (DSC) is another thermal analytical tool which can be used to clarify CD/guest interaction (Mura, 2015; Wadhwa et al., 2017). The volatilization, melting, decomposition, or oxidation peaks can disappear, broaden, or shift as a result of various interaction between components. The inclusion complexation generally raises the shifts, absence or decrease of the endothermic peaks of host or guest molecules (Mura, 2015; Wadhwa et al., 2017). Fig. 6b indicated the DSC graphs of eugenol, γCD powder, nanofibers of pullulan, pullulan/eugenol and pullulan/eugenol-γCD. The DSC graph of pure eugenol had endothermic peak located in the range of 50–210 °C due to the volatilization of eugenol (Fig. 6b) (Choi, Soottitantawat, Nuchuchua, Min, & Ruktanonchai, 2009; Seo, Min, & Choi, 2010). On the other hand, the DSC thermogram of γCD powder and pristine pullulan nanofibers exhibited endothermic peak at ~107 °C and ~97 °C, respectively which were attributed to the dehydration of water (Fig. 6b) (Kowalczyk, Skrzypek, Basiura-Cembala, Łupina, & Mężyńska, 2020; Neacș;u, 2018). The incorporation of active compound into the electrospun nanofibers might induce the shift of thermal transition temperature of the polymer to the lower temperature (Aydogdu et al., 2019). Correspondingly, we observed that the thermal transition of dehydration shifted solely to lower temperature (~87 °C) in case of pullulan/eugenol nanofibers

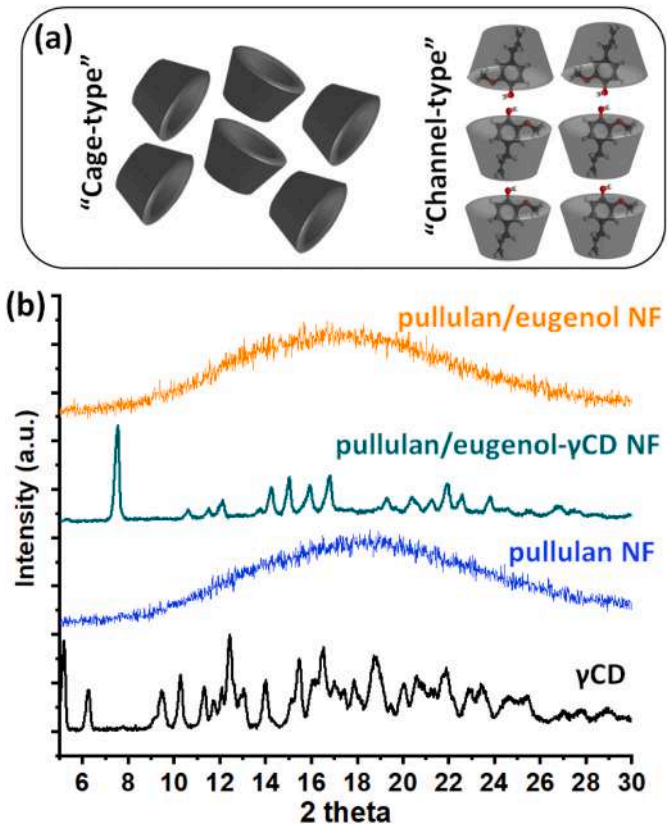

Fig. 5. (a) The schematic representation of the "cage-type" and "channel-type" crystal packing of γCD and eugenol-γCD inclusion complexes, respectively. (b) XRD patterns γCD, pullulan nanofibers (NF), pullulan/eugenol-γCD nanofibers (NF) and pullulan/eugenol nanofibers (NF).

compared to pure pristine pullulan nanofibers. The possible reason for this difference might be the trace amount of volatile eugenol molecules which distributed through the pullulan matrix and made interaction in a sort of way. In case of pullulan/eugenol-γCD nanofibers, the DSC thermogram differentiated so as to reflect both pullulan and γCD profile (Fig. 6b). The peak of the water dehydration has shifted to higher temperature of 102 °C for pullulan/eugenol-γCD nanofibers and has taken place between the thermal transition value of pullulan nanofibers (~97 °C) and γCD (~107 °C) due to the physical blending of these two main components. The thermal transition profile of eugenol in pullulan/eugenol-γCD nanofibers was not obvious in a separate way since it has been already encapsulated into CD cavity.

3.3. Encapsulation efficiency

The native CDs, particularly β- and γ-tend to form inclusion complexes with eugenol having 1:1 M ratio (eugenol:CD) (Piletti et al., 2017; Sebaaly, Charcosset, Stainmesse, Fessi, & Greige-Gerges, 2016; Yang, 2005). In one of the related studies, Yang et al. has used 10:1 M ratio (eugenol:CD) for the preparation of the inclusion complexes of eugenol and various CD types, and the ultimate molar ratio was found 1:1 for the solid-state complexes of βCD and γCD (Yan Yang, 2005). In our study, we have prepared electrospinning systems by the initial eugenol content of 12% (w/w) which corresponded to the molar ratio of 2:1 eugenol:γCD. Here, the high loading of eugenol did not lead to difficulties such as dropping of electrospinning solution or lack of jet stretching during the electrospinning of both eugenol and eugenol-γCD inclusion complex incorporated systems. The encapsulation efficiency of sample was calculated by dissolving pullulan/eugenol and pullulan/eugenol-γCD nanofibers in DMSO. It was found that, pullulan/eugenol and pullulan/eugenol-γCD nanofibers were produced having encapsulation efficiency of 22.5 ± 3.2% and 92.2 ± 1.2% which corresponds to the loading capacity of 2.6 ± 0.4% (w/w) and 10.9 ± 0.1% (w/w), respectively. These results are correlated with the ^{1}H NMR findings where the eugenol content of pullulan/eugenol and pullulan/eugenol-γCD nanofibers were calculated as ~3% and ~11%,

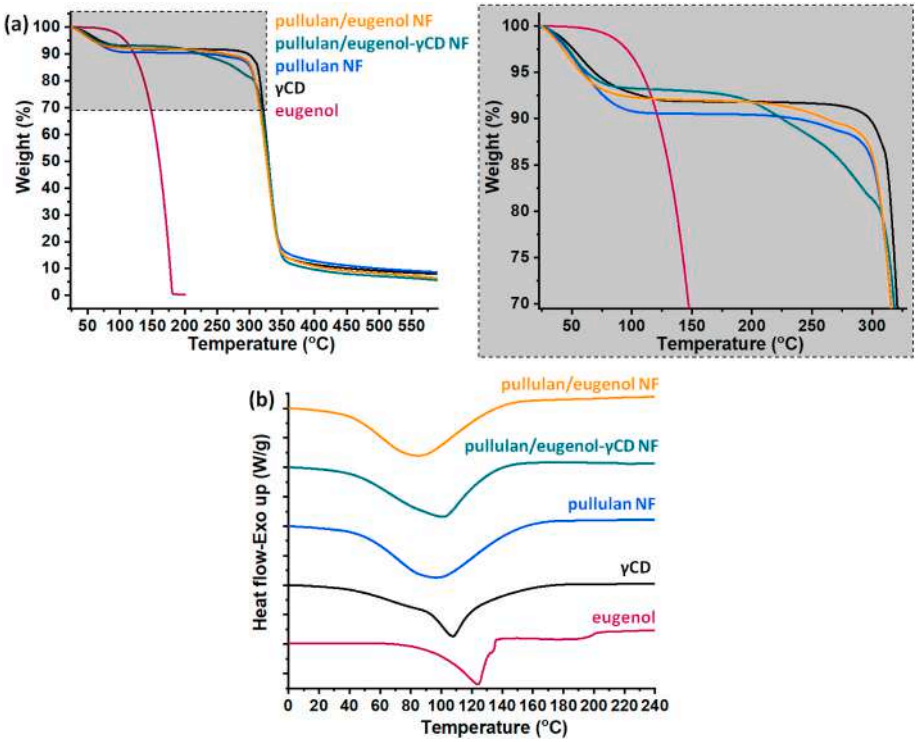

Fig. 6. (a) TGA and (b) DSC thermograms of eugenol, γCD, pullulan nanofibers (NF), pullulan/eugenol-γCD nanofibers (NF) and pullulan/eugenol nanofibers (NF).

respectively. As is seen, the huge amount eugenol was preserved for pullulan/eugenol-γCD nanofibers due to the encapsulation of eugenol molecules into γCD cavities by inclusion complexation. On the other hand, most of the eugenol was lost in case of pullulan/eugenol nanofibers during the preparation and electrospinning steps, because the un-complexed state of eugenol easily evaporated from the polymeric matrix due to its high volatile nature. In another related studies reported by Kayaci et al. similar findings have been observed and the essential oil could not be protected in case of poly(vinyl alcohol) (PVA) nanofibers without inclusion complexes (Kayaci et al., 2013; Kayaci, Sen, Durgun, & Uyar, 2014). The encapsulation efficiency of nanofibrous webs were also analyzed after 3 months storage at room temperature. It was observed that, 18.7 ± 2.8% and 78.2 ± 1.6% of the initial eugenol amount was preserved in pullulan/eugenol and pullulan/eugenol-γCD nanofibers, respectively. Moreover, pullulan/eugenol and pullulan/eugenol-γCD nanofibers were exposed to 175 °C for 1 h and the remained eugenol amount was determined as 10.1 ± 0.1% and 63.0 ± 2.3% of the initial amount, respectively. In other words, pullulan/eugenol-γCD nanofibers contain 9.2 ± 0.2% (w/w) and 7.5 ± 0.3% (w/w) of eugenol after the prolong storage and heat treatment, respectively. On the other hand, only 2.2 ± 0.3% (w/w) and 1.1 ± 0.1% (w/w) of eugenol was preserved in pullulan/eugenol nanofibers after the storage and heat treatment, respectively. The small amount of eugenol remained in the pullulan/eugenol nanofibers might be due to the possible interaction between eugenol and polymeric matrix which we have already discussed in DSC results based on the thermal transition shift of pullulan in case of pullulan/eugenol nanofibers. These results elucidated that, the inclusion complexation ensured high encapsulation efficiency for eugenol during the preparation of solutions and the electrospinning of nanofibers. Additionally, prolong storage and high thermal stability of eugenol can be provided using this approach. It is noteworthy that there is a significant variation between samples according to statistical analyses ($p < 0.05$).

3.4. Time dependent release profile

The release of eugenol from pullulan/eugenol and pullulan/eugenol-γCD nanofibers were studied and the release profiles were shown in Fig. 7. Pullulan/eugenol and pullulan/eugenol-γCD nanofibers reached the maximum released concentration of 38.6 ± 3.4 μg/mL and 164.7 ± 2.5 μg/mL in the 1 and 10 min, respectively and then steady state profile was observed for both sample up to 45 min (Fig. 7). This finding revealed that the both nanofibrous web released ~99% of the loaded eugenol into the dissolution medium. The initial fast release stage happened in the first 1 and 10 min was owing to the complete dissolution of the nanofibers in water. As is seen, the rate of eugenol release from pullulan/eugenol-γCD nanofibers was slower than pullulan/eugenol nanofibers at the initial stage. The different solubility of pristine pullulan and pullulan/inclusion complex matrix was probably the main reason for the differences of initial release rate between two nanofiber systems. As it was explained in the experimental section, the inclusion complex system was prepared using the upper solubility limit of γCD (23%, w/v) (Li et al., 2007). Therefore, the inclusion complex crystals were obtained as a precipitation right after the interaction between eugenol and γCD. Since the pullulan/eugenol-γCD nanofibers were composed of the less soluble inclusion complex form by ~50% (w/w), pullulan/eugenol nanofibers indicated faster initial release of eugenol by dissolution of more soluble pullulan matrix. The release test findings also confirmed the lower eugenol content of pullulan/eugenol nanofibers compared to pullulan/eugenol-γCD nanofibers. Because, the nanofibers of pullulan/eugenol (38.6 ± 3.4 μg/mL) released lower amount of eugenol than pullulan/eugenol-γCD (164.7 ± 2.5 μg/mL) for the same nanofibrous web amount (~60 mg) and the statistical analyses also demonstrated the significant variations between two samples ($p < 0.05$). Here, different kinetic models were used to examine the release profile of samples and the R^2 (correlation coefficient) values were

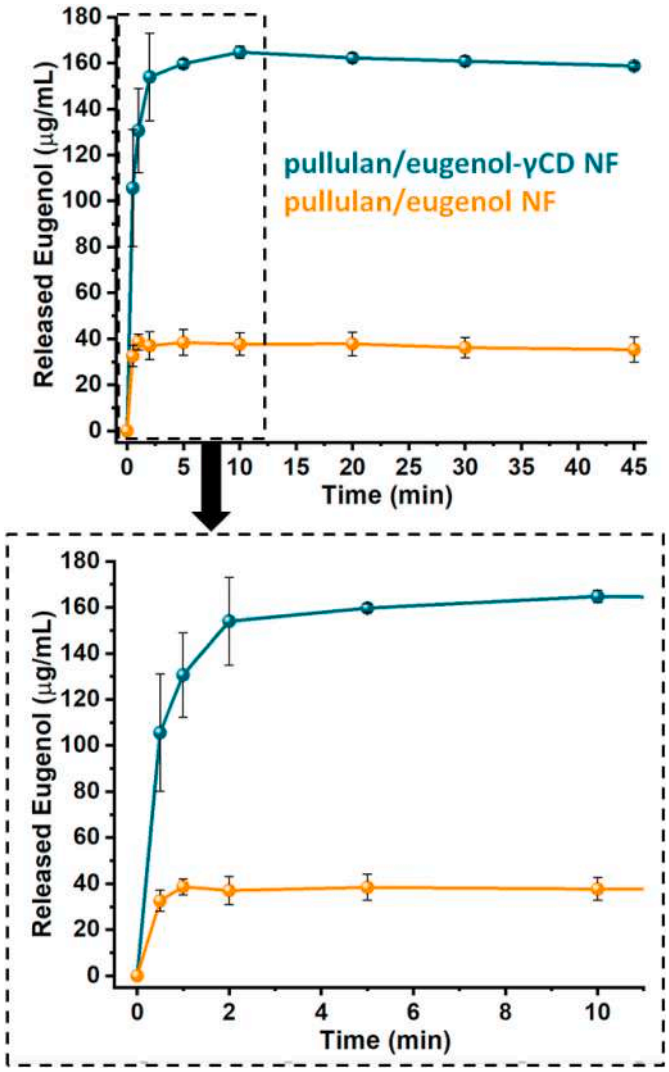

Fig. 7. Time dependent release profiles of pullulan/eugenol-γCD nanofibers (NF) and pullulan/eugenol nanofibers (NF).

summarized in Table S1. The R^2 values showed that, the release of eugenol from pullulan/eugenol nanofiber was not compatible with zero/first-order kinetics and Higuchi model. On the other hand, the release profile of pullulan/eugenol-γCD nanofibers was fitted with the first-order kinetics due to high R^2 value of 0.95, but it was not correlated with both zero-order kinetics and Higuchi model. These results suggested that, for both electrospun nanofibrous webs, the release of eugenol did not arise from a planar matrix which did not dissolve in water (Fick's first law) (Peppas & Narasimhan, 2014). However, the high R^2 value of the first-order kinetic depicted that the eugenol was inclined to release in a time dependent manner in case of pullulan/eugenol-γCD nanofibers (Peppas & Narasimhan, 2014). Both nanofibrous webs indicated relatively higher consistency with Korsmeyer–Peppas model and the diffusion exponent (n) value was also determined (Table S1). The n values of both samples were detected in the $0.45 < n < 0.89$ range and it demonstrated the non-Fickian or irregular diffusion of eugenol from the sample by erosion-controlled and diffusion based release (Li, Kanjwal, Lin, & Chronakis, 2013; Peppas & Narasimhan, 2014). In another related study, the n values were also found in the same range of $0.45 < n < 0.89$ for the caffeine/riboflavin loaded PVA nanofibers which had hydrophilic nature and so fast-dissolving property in water (Li et al., 2013). Briefly, the 3D continuous feature, porosity, high surface area of nanofibrous webs and

the hydrophilic nature of pullulan and γCD facilitated the wetting and dissolution of the electrospun samples by increasing the penetration way and the contact sides for water. Moreover, inclusion complex crystals incorporated into the nanofibrous webs provided a slower initial release with a relatively more controlled manner for encapsulated eugenol compared to pristine eugenol incorporated pullulan nanofibers.

3.5. Antioxidant activity

Eugenol is a phenolic compound in which the antioxidant activity occurs by the removing of a hydrogen atom from its phenol donor to the radical acceptor. The aromatic ring of eugenol stabilizes the scavenged radical with its conjugated structure which also improves the antioxidant efficiency of eugenol (Bezerra et al., 2017; Gülçin, 2012). In this study, we have used DPPH assay in order to evaluate the antioxidant potential of our samples. Here, the antioxidant activity of the pullulan/eugenol-γCD nanofibers was evaluated for the different nanoweb concentrations ranging at 4–250 μg/mL. For the control experiment, the antioxidant test was also performed for pullulan/eugenol nanofibers using the same sample concentration range. Fig. 8a displayed the radical inhibition (%) graphs of pullulan/eugenol and pullulan/eugenol-γCD nanofibers depending on the concentration and the representative photos of all systems. As expected, the antioxidant activity of both samples increased against increasing nanoweb concentration owing to dosage dependent scavenging behaviour. For the highest sample concentration, pullulan/eugenol-γCD nanofibers indicated 100 ± 0.0% radical scavenging performance. On the other hand, pullulan/eugenol nanofibers inhibited 58.1 ± 8.1% of the DPPH radicals for the same sample concentration of 250 μg/mL. The photo of the systems also supported this finding where the colour of the solution of pullulan/eugenol-γCD sample completely turned into yellow, while the solution of pullulan/eugenol sample indicated purple hue (Fig. 8a). Moreover, pullulan/eugenol-γCD nanofiber indicated some radical scavenging activity (1.3 ± 2.3%) for the lowest nanofiber concentration (4 μg/mL). On the other hand, there is no recorded antioxidant activity for the 4 μg/mL concentrated solution of pullulan/eugenol nanofibers (Fig. 8a). As it was addressed in the encapsulation efficiency test and release profile, pullulan/eugenol-γCD nanofiber have been obtained having higher eugenol content (10.9 ± 0.1% (w/w)) compared to pullulan/eugenol nanofibers (2.6 ± 0.4% (w/w)). Therefore, higher amount of eugenol took part in the radical inhibition process in case of pullulan/eugenol-γCD nanofibers, and so it displayed significantly better antioxidant activity than pullulan/eugenol nanofibers for the same amount of nanofibrous webs. The antioxidant activity of pristine pullulan nanofiber and γCD was also carried out, however both did not indicate radical scavenging activity (data is not given).

The substance concentration needed to inhibit the 50% of initial DPPH radical concentration (IC50) was also determined using the concentration dependent radical scavenging graphs of samples (Ak & Gülçin, 2008). The IC50 value for pullulan/eugenol nanofibers and pullulan/eugenol-γCD nanofibers were found as the nanoweb concentration of ~230 μg/mL and ~29 μg/mL, respectively. It is obvious from this finding, pullulan/eugenol-γCD nanofibers had superior antioxidant activity due its higher encapsulation efficiency and therefore, less amount of nanofibrous web was needed than pullulan/eugenol nanofibers in order to attain antioxidant property. As it was previously discussed, the antioxidant property of eugenol molecule depends on its phenolic structure. This phenolic group is situated to the wider rim of the CD molecule during inclusion complexation (Nuchuchua et al., 2009) and this localization is not supposed to inhibit the radical scavenging property of eugenol compound (Celebioglu et al., 2018b; Cetin Babaoglu, Bayrak, Ozdemir, & Ozgun, 2017). Due to this localization,

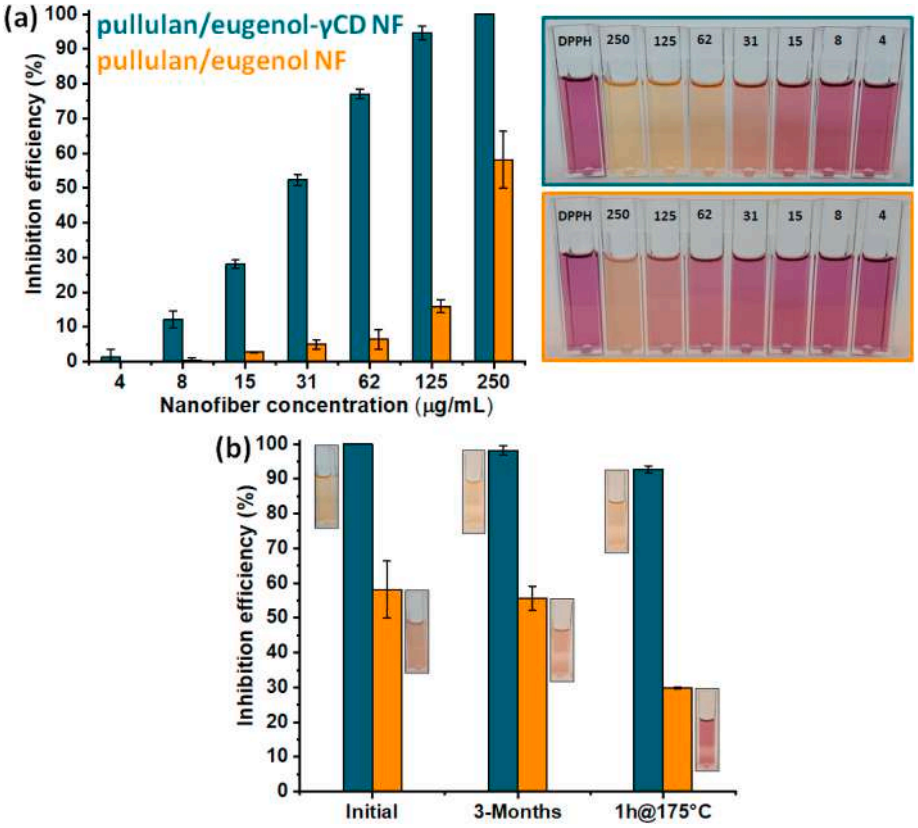

Fig. 8. (a) Concentration dependent antioxidants performance graphs and the representative solution photos of pullulan/eugenol-γCD nanofibers (NF) and pullulan/eugenol nanofibers (NF). (b) The antioxidants performance graphs of pullulan/eugenol-γCD nanofibers (NF) and pullulan/eugenol nanofibers before and after the long-term storage (3-months) and thermal treatment (175 °C for 1 h) for the highest sample concentration of 250 μm/mL.

we have not observed any hindrance of the antioxidant activity of eugenol molecules for the eugenol-γCD inclusion complex incorporated pullulan nanofibers. Here, the antioxidant test was also conducted for the electrospun nanofibers which were kept at room temperature for 3 months or exposed heat treatment at 175 °C for 1 h. The highest nanoweb concentration (250 μg/mL) was used for the mentioned tests and the inhibition efficiency graphs were depicted in Fig. 8b. After the 3 months storage, the inhibition efficiency value of pullulan/eugenol and pullulan/eugenol-γCD nanofibers were determined as 55.6 ± 3.5% and 98.2 ± 1.4%, respectively. As is seen, there was not a significant difference of inhibition activity for both samples compared to their initial state. This result was correlated with the findings of encapsulation efficiency test in which the eugenol content of the electrospun nanofibers did not change significantly by the end of 3 months. On the other side, the thermally treated samples (175 °C for 1 h) of pullulan/eugenol and pullulan/eugenol-γCD nanofibers depicted antioxidant activity with the inhibition efficiency of 29.8 ± 0.2% and 92.8 ± 1.0%, respectively. Even, the results were correlated with the encapsulation efficiency findings, the radical scavenging activity of pullulan/eugenol nanofibers decreased more distinctly than pullulan/eugenol-γCD nanofibers. The reason might be the enhanced thermal stability of eugenol molecules in pullulan/eugenol-γCD nanofibers by inclusion complexation which was also confirmed by the TGA analysis. In brief, the higher encapsulation efficiency of pullulan/eugenol-γCD nanofibers enabled to obtain quite effective antioxidant activity using significantly less amount of nanofibrous web compared to pullulan/eugenol nanofibers. Moreover, pullulan/eugenol-γCD nanofibers provided a sustainable radical scavenging activity under the circumstances of prolong storage and high temperature. Here, $p < 0.05$ value of statistical analyses depicted the significant variations between samples.

4. Conclusion

To conclude, electrospinning is a feasible technique in order to develop a free-standing encapsulation and carrying matrix for the active compounds which are widely used in food and pharmaceutical industries. This technique allows to produce nanofibers from a large range of materials including the biopolymer of polysaccharides and their composites with other components. So, electrospinning enables to obtain sustainable materials by eliminating the environmental and health loadings originating from the use of synthetic products. On the one part, natural and non-toxic cyclodextrin molecules enable to improve the stability and solubility of the concerned active compounds by forming inclusion complexes. Thus, the integration of the phenomenon of electrospinning and cyclodextrin paves the way to form promising materials having the advantages parts of both electrospun nanofibers and cyclodextrin molecules. From this point view, here we have formed the inclusion complexes of γCD and highly volatile essential oil compound of eugenol and we have used the microbial polysaccharides of pullulan as a polymeric matrix for the electrospinning. The composite pullulan/eugenol-γCD nanofibers were fabricated in one-step process without an additional step. The free-standing nanofibrous webs of pullulan/eugenol and pullulan/eugenol-γCD were obtained with ~525 nm and ~260 nm average diameter, respectively. The inclusion complexation provided a distinctively high preservation yield for the volatile eugenol molecules and the ultimate nanofibers were obtained by ~93% encapsulation efficiency. On the other hand, only ~23% of eugenol was able to be protected without complexation in the pullulan nanofibers. This enhanced yield has showed its effect on the antioxidant activity, as well. We observed that, less amount of nanofibrous web is enough to reach an effective antioxidant property for pullulan/eugenol-γCD systems (IC50; ~29 μg/mL) compared to pullulan/eugenol one (IC50; ~230 μg/mL). The antioxidant activity of eugenol was effectively kept even after long-term storage (98.2 ± 1.4%, 3-months) and heat-treatment (92.8 ± 1.0%, 175 °C for 1 h) for pullulan/eugenol-γCD nanofibers. The inclusion complexation also provided an enhanced thermal stability for eugenol and the volatilization of eugenol shifted from the range of ~50–190 °C to ~125–300 °C in case of pullulan/eugenol-γCD nanofibers. Pullulan/eugenol-γCD nanofibers indicated difference also during the release of eugenol and provided a relatively controlled manner release compared to pristine eugenol included pullulan nanofibers. It is worth to state that, the electrospinning was carried out using water and this also offers a non-negligible advantage for the industrial scale commercialization of the inclusion complex incorporated nanofibers. In short, there is a huge demand of consumers for the natural and safe alternatives against synthetic ones. In this respect, the edible pullulan polymer which is in the form of flexible and free-standing nanofibrous webs and incorporated with the antioxidant eugenol-γCD inclusion complexes can be quite promising for food and pharmaceutical applications. This attractive design can pave the way for the development of novel food packaging materials. Moreover, these functional strip/web structures can have potential as food/dietary supplements or can be incorporated into medical patches depending on the scope of practices.

CRediT authorship contribution statement

Asli Celebioglu: Conceptualization, Methodology, Validation, Investigation, Writing - original draft, Writing - review & editing. **Tamer Uyar:** Supervision, Resources, Conceptualization, Methodology, Project administration, Funding acquisition.

Declaration of competing interest

The authors declare that they have no known competing financial interests or personal relationships that could have appeared to influence the work reported in this paper.

Acknowledgments

This work made use of the Cornell Center for Materials Research Shared Facilities which are supported through the NSF MRSEC program (DMR-1719875), and the Cornell Chemistry NMR Facility supported in part by the NSF MRI program (CHE-1531632), and the Department of Fiber Science & Apparel Design facilities. Prof. Uyar acknowledges the startup funding from the College of Human Ecology at Cornell University. The partial funding for this research was also graciously provided by Nixon Family (Lea and John Nixon) thru College of Human Ecology at Cornell University.

Appendix A. Supplementary data

Supplementary data to this article can be found online at https://doi.org/10.1016/j.foodhyd.2020.106264.

References

Abarca, R. L., Rodriguez, F. J., Guarda, A., Galotto, M. J., & Bruna, J. E. (2016). Characterization of beta-cyclodextrin inclusion complexes containing an essential oil component. *Food Chemistry, 196*, 968–975.

Aceituno-Medina, M., Mendoza, S., Lagaron, J. M., & López-Rubio, A. (2015). Photoprotection of folic acid upon encapsulation in food-grade amaranth (Amaranthus hypochondriacus L.) protein isolate–Pullulan electrospun fibers. *LWT-Food Science and Technology, 62*(2), 970–975.

Ak, T., & Gülçin, İ. (2008). Antioxidant and radical scavenging properties of curcumin. *Chemico-Biological Interactions, 174*(1), 27–37.

Alenezi, H., Cam, M. E., & Edirisinghe, M. (2019). Experimental and theoretical investigation of the fluid behavior during polymeric fiber formation with and without pressure. *Applied Physics Reviews, 6*(4), 41401.

Amorati, R., Foti, M. C., & Valgimigli, L. (2013). Antioxidant activity of essential oils. *Journal of Agricultural and Food Chemistry, 61*(46), 10835–10847.

Aydogdu, A., Yildiz, E., Aydogdu, Y., Sumnu, G., Sahin, S., & Ayhan, Z. (2019). Enhancing oxidative stability of walnuts by using gallic acid loaded lentil flour based electrospun nanofibers as active packaging material. *Food Hydrocolloids, 95*, 245–255.

Barba, C., Eguinoa, A., & Maté, J. I. (2015). Preparation and characterization of β-cyclodextrin inclusion complexes as a tool of a controlled antimicrobial release in whey protein edible films. *LWT-Food Science and Technology, 64*(2), 1362–1369.
Bezerra, D. P., Militão, G. C. G., De Morais, M. C., & De Sousa, D. P. (2017). The dual antioxidant/prooxidant effect of eugenol and its action in cancer development and treatment. *Nutrients, 9*(12), 1367.
Bilensoy, E. (2011). *Cyclodextrins in pharmaceutics, cosmetics, and biomedicine: Current and future industrial applications*. John Wiley & Sons.
Blanco-Padilla, A., López-Rubio, A., Loarca-Pina, G., Gómez-Mascaraque, L. G., & Mendoza, S. (2015). Characterization, release and antioxidant activity of curcumin-loaded amaranth-pullulan electrospun fibers. *LWT-Food Science and Technology, 63*(2), 1137–1144.
Celebioglu, A., Ipek, S., Durgun, E., & Uyar, T. (2017). Selective and efficient removal of volatile organic compounds by channel-type gamma-cyclodextrin assembly through inclusion complexation. *Industrial & Engineering Chemistry Research, 56*(25), 7345–7354.
Celebioglu, A., Yildiz, Z. I., & Uyar, T. (2018a). Electrospun nanofibers from cyclodextrin inclusion complexes with cineole and p-cymene: Enhanced water solubility and thermal stability. *International Journal of Food Science and Technology, 53*(1), 112–120.
Celebioglu, A., Yildiz, Z. I., & Uyar, T. (2018b). Fabrication of electrospun eugenol/cyclodextrin inclusion complex nanofibrous webs for enhanced antioxidant property, water solubility, and high temperature stability. *Journal of Agricultural and Food Chemistry, 66*(2), 457–466.
Celebioglu, A., Yildiz, Z. I., & Uyar, T. (2018c). Thymol/cyclodextrin inclusion complex nanofibrous webs: Enhanced water solubility, high thermal stability and antioxidant property of thymol. *Food Research International, 106*, 280–290.
Cetin Babaoglu, H., Bayrak, A., Ozdemir, N., & Ozgun, N. (2017). Encapsulation of clove essential oil in hydroxypropyl beta-cyclodextrin for characterization, controlled release, and antioxidant activity. *Journal of Food Processing and Preservation, 41*(5), Article e13202.
Choi, M.-J., Soottitantawat, A., Nuchuchua, O., Min, S.-G., & Ruktanonchai, U. (2009). Physical and light oxidative properties of eugenol encapsulated by molecular inclusion and emulsion–diffusion method. *Food Research International, 42*(1), 148–156.
Duan, G., & Greiner, A. (2019). Air-blowing-assisted coaxial electrospinning toward high productivity of Core/sheath and hollow fibers. *Macromolecular Materials and Engineering, 304*(5), 1800669.
Farkas, B., Balogh, A., Cselkó, R., Molnár, K., Farkas, A., Borbás, E., et al. (2019). Corona alternating current electrospinning: A combined approach for increasing the productivity of electrospinning. *International Journal of Pharmaceutics, 561*, 219–227.
García-Moreno, P. J., Özdemir, N., Stephansen, K., Mateiu, R. V., Echegoyen, Y., Lagaron, J. M., … Jacobsen, C. (2017). Development of carbohydrate-based nano-microstructures loaded with fish oil by using electrohydrodynamic processing. *Food Hydrocolloids, 69*, 273–285.
Göttel, B., e Silva, J. M. de S., de Oliveira, C. S., Syrowatka, F., Fiorentzis, M., Viestenz, A., … Mäder, K. (2020). Electrospun nanofibers–A promising solid in-situ gelling alternative for ocular drug delivery. *European Journal of Pharmaceutics and Biopharmaceutics, 146*, 125–132.
Gülçin, I. (2012). Antioxidant activity of food constituents: An overview. *Archives of Toxicology*. https://doi.org/10.1007/s00204-011-0774-2.
Hassan, B., Chatha, S. A. S., Hussain, A. I., Zia, K. M., & Akhtar, N. (2018). Recent advances on polysaccharides, lipids and protein based edible films and coatings: A review. *International Journal of Biological Macromolecules, 109*, 1095–1107.
Islam, M. S., & Yeum, J. H. (2013). Electrospun pullulan/poly (vinyl alcohol)/silver hybrid nanofibers: Preparation and property characterization for antibacterial activity. *Colloids and Surfaces A: Physicochemical and Engineering Aspects, 436*, 279–286.
Jain, R., Shetty, S., & Yadav, K. S. (2020). Unfolding the electrospinning potential of biopolymers for preparation of nanofibers. *Journal of Drug Delivery Science and Technology*, 101604.
Jindal, N., & Khattar, J. S. (2018). Microbial polysaccharides in food industry. In *Biopolymers for food design* (pp. 95–123). Elsevier.
Kayaci, F., Ertas, Y., & Uyar, T. (2013). Enhanced thermal stability of eugenol by cyclodextrin inclusion complex encapsulated in electrospun polymeric nanofibers. *Journal of Agricultural and Food Chemistry, 61*(34), 8156–8165.
Kayaci, F., Sen, H. S., Durgun, E., & Uyar, T. (2014). Functional electrospun polymeric nanofibers incorporating geraniol–cyclodextrin inclusion complexes: High thermal stability and enhanced durability of geraniol. *Food Research International, 62*, 424–431.
Kowalczyk, D., Skrzypek, T., Basiura-Cembala, M., Łupina, K., & Mężyńska, M. (2020). The effect of potassium sorbate on the physicochemical properties of edible films based on pullulan, gelatin and their blends. *Food Hydrocolloids*, 105837.
Li, X., Kanjwal, M. A., Lin, L., & Chronakis, I. S. (2013). Electrospun polyvinyl-alcohol nanofibers as oral fast-dissolving delivery system of caffeine and riboflavin. *Colloids and Surfaces B: Biointerfaces, 103*, 182–188.
Li, Z., Wang, M., Wang, F., Gu, Z., Du, G., Wu, J., et al. (2007). γ-Cyclodextrin: A review on enzymatic production and applications. *Applied Microbiology and Biotechnology, 77*(2), 245.
Llana-Ruiz-Cabello, M., Pichardo, S., Maisanaba, S., Puerto, M., Prieto, A. I., Gutierrez-Praena, D., … Camean, A. M. (2015). In vitro toxicological evaluation of essential oils and their main compounds used in active food packaging: A review. *Food and Chemical Toxicology, 81*, 9–27.
Mahalingam, S., Homer-Vanniasinkam, S., & Edirisinghe, M. (2019). Novel pressurised gyration device for making core-sheath polymer fibres. *Materials & Design, 178*, 107846.
Mascheroni, E., Fuenmayor, C. A., Cosio, M. S., Di Silvestro, G., Piergiovanni, L., Mannino, S., et al. (2013). Encapsulation of volatiles in nanofibrous polysaccharide membranes for humidity-triggered release. *Carbohydrate Polymers, 98*(1), 17–25.
Mura, P. (2015). Analytical techniques for characterization of cyclodextrin complexes in the solid state: A review. *Journal of Pharmaceutical and Biomedical Analysis, 113*, 226–238.
Neacşu, A. (2018). Physicochemical investigation of the complexation between γ-cyclodextrin and doxorubicin in solution and in solid state. *Thermochimica Acta, 661*, 51–58.
Nuchuchua, O., Saesoo, S., Sramala, I., Puttipipatkhachorn, S., Soottitantawat, A., & Ruktanonchai, U. (2009). Physicochemical investigation and molecular modeling of cyclodextrin complexation mechanism with eugenol. *Food Research International, 42*(8), 1178–1185.
Peppas, N. A., & Narasimhan, B. (2014). Mathematical models in drug delivery: How modeling has shaped the way we design new drug delivery systems. *Journal of Controlled Release, 190*, 75–81.
Piletti, R., Bugiereck, A. M., Pereira, A. T., Gussati, E., Dal Magro, J., Mello, J. M. M., … Riella, H. G. (2017). Microencapsulation of eugenol molecules by β-cyclodextrine as a thermal protection method of antibacterial action. *Materials Science and Engineering: C, 75*, 259–271.
Qin, Z., Jia, X.-W., Liu, Q., Kong, B., & Wang, H. (2019). Fast dissolving oral films for drug delivery prepared from chitosan/pullulan electrospinning nanofibers. *International Journal of Biological Macromolecules, 137*, 224–231.
Román, J. T., Fuenmayor, C. A., Dominguez, C. M. Z., Clavijo-Grimaldo, D., Acosta, M., García-Castañeda, J. E., … Rivera-Monroy, Z. J. (2019). Pullulan nanofibers containing the antimicrobial palindromic peptide LfcinB (21–25) Pal obtained via electrospinning. *RSC Advances, 9*(35), 20432–20438.
Sebaaly, C., Charcosset, C., Stainmesse, S., Fessi, H., & Greige-Gerges, H. (2016). Clove essential oil-in-cyclodextrin-in-liposomes in the aqueous and lyophilized states: From laboratory to large scale using a membrane contactor. *Carbohydrate Polymers, 138*, 75–85.
Seethu, B. G., Pushpadass, H. A., Emerald, F. M. E., Nath, B. S., Naik, N. L., & Subramanian, K. S. (2020). Electrohydrodynamic encapsulation of resveratrol using food-grade nanofibres: Process optimization, characterization and fortification. *Food and Bioprocess Technology, 13*(2), 341–354.
Seo, E.-J., Min, S.-G., & Choi, M.-J. (2010). Release characteristics of freeze-dried eugenol encapsulated with β-cyclodextrin by molecular inclusion method. *Journal of Microencapsulation, 27*(6), 496–505.
Shao, P., Niu, B., Chen, H., & Sun, P. (2018). Fabrication and characterization of tea polyphenols loaded pullulan-CMC electrospun nanofiber for fruit preservation. *International Journal of Biological Macromolecules, 107*, 1908–1914.
Sharma, N., & Baldi, A. (2016). Exploring versatile applications of cyclodextrins: An overview. *Drug Delivery, 23*(3), 729–747.
Shibata, M., Asahina, M., Teramoto, N., & Yosomiya, R. (2001). Chemical modification of pullulan by isocyanate compounds. *Polymer, 42*(1), 59–64.
Singh, R. S., Kaur, N., & Kennedy, J. F. (2015). Pullulan and pullulan derivatives as promising biomolecules for drug and gene targeting. *Carbohydrate Polymers, 123*, 190–207.
Singh, R. S., Kaur, N., & Kennedy, J. F. (2019). *Pullulan production from agro-industrial waste and its applications in food industry: A review*. Carbohydrate Polymers.
Singh, R. S., Kaur, N., Rana, V., & Kennedy, J. F. (2017). Pullulan: A novel molecule for biomedical applications. *Carbohydrate Polymers, 171*, 102–121.
Song, L. X., Xu, P., Wang, H. M., & Yang, Y. (2009). Inclusion phenomena of clove oil with α-, β-, γ-and heptakis (2, 6-di-O-methyl)-β-cyclodextrin. *Natural Product Research, 23*(9), 789–800.
Soto, K. M., Hernández-Iturriaga, M., Loarca-Piña, G., Luna-Bárcenas, G., & Mendoza, S. (2019). Antimicrobial effect of nisin electrospun amaranth: Pullulan nanofibers in apple juice and fresh cheese. *International Journal of Food Microbiology, 295*, 25–32.
Stijnman, A. C., Bodnar, I., & Tromp, R. H. (2011). Electrospinning of food-grade polysaccharides. *Food Hydrocolloids, 25*(5), 1393–1398.
Sugumaran, K. R., & Ponnusami, V. (2017). Review on production, downstream processing and characterization of microbial pullulan. *Carbohydrate Polymers, 173*, 573–591.
Trinetta, V., & Cutter, C. N. (2016). Pullulan: A suitable biopolymer for antimicrobial food packaging applications. In *Antimicrobial food packaging* (pp. 385–397). Elsevier.
Uyar, T., & Besenbacher, F. (2008). Electrospinning of uniform polystyrene fibers: The effect of solvent conductivity. *Polymer, 49*(24), 5336–5343.
Wadhwa, G., Kumar, S., Chhabra, L., Mahant, S., & Rao, R. (2017). Essential oil–cyclodextrin complexes: An updated review. *Journal of Inclusion Phenomena and Macrocyclic Chemistry, 89*(1–2), 39–58.
Wang, T., Li, B., Si, H., Lin, L., & Chen, L. (2011). Release characteristics and antibacterial activity of solid state eugenol/β-cyclodextrin inclusion complex. *Journal of Inclusion Phenomena and Macrocyclic Chemistry, 71*(1–2), 207–213.
Xue, J., Wu, T., Dai, Y., & Xia, Y. (2019). Electrospinning and electrospun nanofibers: Methods, materials, and applications. *Chemical Reviews, 119*(8), 5298–5415.
Yadav, H., & Karthikeyan, C. (2019). Natural polysaccharides: Structural features and properties. In *Polysaccharide carriers for drug delivery* (pp. 1–17). Elsevier.
Yang, Y. (2005). Study on the inclusion compounds of eugenol with α-, β-, γ-and heptakis (2, 6-di-O-methyl)-β-cyclodextrins. *Journal of Inclusion Phenomena and Macrocyclic Chemistry, 53*(1–2), 27–33.

Yang, Y., Xie, B., Liu, Q., Kong, B., & Wang, H. (2020). Fabrication and characterization of a novel polysaccharide based composite nanofiber films with tunable physical properties. *Carbohydrate Polymers, 236*, 116054.
Yildiz, Z. I., Celebioglu, A., Kilic, M. E., Durgun, E., & Uyar, T. (2018). Fast-dissolving carvacrol/cyclodextrin inclusion complex electrospun fibers with enhanced thermal stability, water solubility, and antioxidant activity. *Journal of Materials Science, 53* (23), 15837–15849.
Zhu, Y., Romain, C., & Williams, C. K. (2016). Sustainable polymers from renewable resources. *Nature, 540*(7633), 354–362.